

DETC2014-34661

CASCADED PREDICTIVE CONTROL OF TIRE FORCE SATURATION LEVELS FOR VEHICLE STABILITY

Justin Sill
Tesla Motors
Palo Alto, CA, USA

Beshah Ayalew
Clemson University- International Center for
Automotive Research
Greenville, SC, USA

ABSTRACT

This paper proposes and demonstrates a cascaded predictive control strategy that quantifies and uses longitudinal and lateral tire force saturation for directional stability control of road vehicles. Saturation is explicitly defined and computed as the deficiency of a tire to generate a linearly increasing force in either the lateral or longitudinal direction. The optimal management of lateral saturation levels is set as the objective for an upper level controller, while the optimal management of longitudinal saturation among all tires is set as the objective for a lower level driving/braking torque distribution controller. This cascaded predictive scheme exploits prevailing time scale separations between the lateral vehicle dynamics and the tire/wheel dynamics. The performance of the approach is illustrated using simulations of a medium-duty truck undergoing a transient handling maneuver.

INTRODUCTION

Vehicle stability control (VSC) systems reduce accident rates by helping drivers maintain control over the vehicle during emergency/aggressive maneuvers near the limits of tire/road adhesion[1]. Most commercial VSC systems accomplish this through rule-based differential braking on either the front or rear wheels to generate the corrective yaw moment needed for stabilization or for achieving driver's directional intention [1, 2]. In this work, we target the optimal use of available tire force generation capability through optimal distribution of driving or braking torque to each wheel of the vehicle. This approach is suited to emerging electric and hybrid vehicles with independent drive arrangements. In[3, 4], an optimal yaw moment controller was proposed for such a vehicle. This works and others in [5, 6] first determine stabilizing yaw moments based on errors of actual vehicle responses from reference/desired yaw rates and/or lateral accelerations predicted using a linear model of the vehicle. The yaw moments are then set to be achieved with pre-determined torque distribution rules.

Our approach is a model predictive control (MPC) structure that stabilizes the vehicle with balanced use of all tires. In

recent years, there has been increasing interest in application of MPC to vehicle control. In [7-10], MPC techniques have been applied with steering and braking actuation to achieve path-tracking objectives for autonomous/robotic vehicles. Specifically, the application of linear MPC and quadratic programming with linear constraints was shown to provide optimal performance, while maintaining sufficiently low computation times. In [11], MPC was proposed for vehicle stability control with corrective braking (no drive torque) on a vehicle. However, the approach described relies on the pre-determination of a reference/desired yaw rate and side-slip angle using steady-state yaw rate and side slip angle gains of a single-track vehicle model. In [12], MPC is proposed for traction control systems, where the MPC objective involved limiting the estimated wheel slip velocity of the driven wheels over a selected prediction horizon. A noteworthy aspect of the work in [12] is the use of a piecewise linear tire-force curve for purposes of identifying and switching between two parameterized linear prediction models. Our approach of quantifying and using tire saturation avoids the necessity of switching between such models.

In this work, we propose an MPC approach that is implemented as a two-level cascade to handle both the low-level torque distribution and the high-level yaw moment generation by explicitly taking into account the nonlinearities of tire force saturation. Our approach relies on the use of standard sensor information readily available on-board modern vehicles (wheel speeds, yaw rate, lateral acceleration). We also rely on tire force and slip angle estimation schemes that have already been widely proposed and demonstrated in the literature. For the sake of brevity, we refer the reader to the following sources on the topics of longitudinal and lateral tire force estimation as well as estimations of slip angles and forward velocities [2, 13-16, 23]. In addition, our discussion assumes independent drive architectures that are capable of generating both driving and (regenerative) braking torques. However, with some modifications of the relevant optimization constraints, the ideas can be extended to brake-based systems

and “torque-vectoring” active differentials within conventional powertrains [17, 18].

The rest of this paper is organized as follows. First we give the motivation and definitions for the proposed saturation control. Then, we discuss the mathematical details of the proposed cascaded predictive saturation management scheme. Finally, we give demonstrative simulation results and offer brief conclusions.

NOMENCLATURE

A, B, C, E	Linearized model matrices
A_{eq}, B_{eq}	Equality constraint matrices
b_i	Viscous wheel damping
C_D	Aerodynamic drag coefficient
C_a	Lateral cornering stiffness
C_x	Longitudinal slip stiffness
d_f	Front track width
d_r	Rear track width
$\Delta E_{kinetic}$	Change in kinetic energy
E_{loss}	Energy loss due to tires
FMVSS	Federal Motor Vehicle Safety Standards
F_x	Longitudinal tire force
$F_{y,f}$	Front axle lateral force
$F_{y,r}$	Rear axle lateral force
I_w	Tire/wheel rotational inertia
J	Cost/objective function
J_z	Vehicle yaw inertia
K_1, K_2	Tire property coefficients
l_f	Distance from CG to front axle
l_r	Distance from CG to rear axle
m	Vehicle mass
M_ψ	Corrective yaw moment
Q_l	Instant weighting matrix for low-level MPC
Q	Expanded weighting matrix for low-level MPC
$Q_{a,l}$	Instant weighting matrix for high-level MPC
Q_a	Expanded weighting matrix for high-level MPC
R_w	Tire Radius
S	Frontal Area
T_i	Individual wheel torque
u	Control input
Δu	Control input increment
U	Expanded control input for prediction
ΔU	Expanded control input increment for control horizon
VSC	Vehicle Stability Control
V_x	Longitudinal vehicle velocity
V_y	Lateral vehicle velocity
x	Predicted state vector
y	Predicted output vector
Y	Predicted output vector for entire prediction horizon
α	Lateral slip angle
α_{sat}	Lateral tire saturation
γ, ζ, Ω	Prediction matrices
δ	Road wheel steering
ψ	yaw angle
κ	Longitudinal tire saturation
σ	Longitudinal slip ratio

ρ Air density
 ω_i Individual wheel spin

DEFINITION AND MOTIVATION FOR SATURATION CONTROL

Definition of Tire Force Saturation

We define and interpret saturation as the deficiency of the tire to generate a linearly increasing tire force with increasing slip (Figure1).

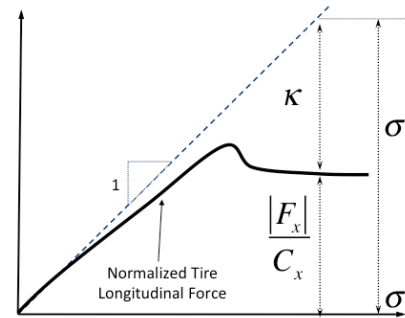


Figure 1 Definition of longitudinal tire force saturation

Specifically, the longitudinal tire force saturation is defined as follows:

$$\kappa_i = \sigma_i - \frac{F_{x,i}}{C_{x,i}} \quad (1)$$

where, σ_i is the tire/wheel longitudinal slip ratio; $F_{x,i}$ is the longitudinal tire force; and $C_{x,i}$ is the slip stiffness of the tire. Saturation of the lateral force can be defined similarly. For the purposes of this paper, only the per-axle lateral force saturations are relevant and are defined by:

$$\alpha_{sat} = \alpha - \frac{F_y}{C_a} \quad (2)$$

where, α is the (front or rear) axle slip angle, F_y is the axle lateral force and C_a is the axle cornering stiffness. We again note that both the forces and slip quantities are assumed to be known via one or more of the various estimation methods, some of which are cited earlier.

Motivation and Application to Vehicle Stability Control

The basic notion we exploit is that saturating tires are inefficient in transmitting the necessary forces for stabilizing a road vehicle or for basic traction control. In fact, current ABS and TCS systems apply interventions to avoid operation in saturating regimes at all tires. In Limroth [19], saturation is treated as a discontinuous quantity whereby the first significant deviations from the linear projection are used as a cue to activate braking interventions to the axle deemed to be saturating. Our conjecture is that saturation can be treated as continuous quantity that can be optimally managed to efficiently use all tires on the vehicle. In our previous work[20, 21], the differences in the lateral saturation levels between the front and the rear axles were used to construct a PI type yaw moment controller that successfully stabilized the vehicle. We also showed [20] that the saturation balancing approach imbeds

'internal' surface and tire-capability dependent reference response. In [21], we introduced the model predictive torque distribution strategy to optimally balance longitudinal saturations at the low level while working with the PI type yaw moment controller at the high level. In this paper, we extend these ideas by formulating a cascaded predictive structure that manages *both* the longitudinal and lateral saturation levels among all the tires to influence the directional stability of the vehicle.

PREDICTIVE SATURATION MANAGEMENT

Cascaded Predictive Vehicle Stability Control

Figure 2 outlines the proposed scheme.

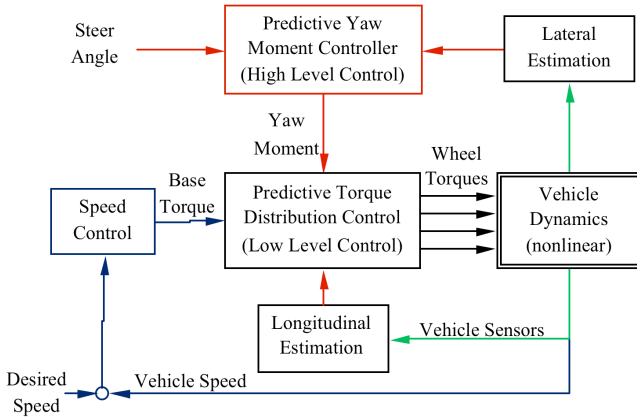


Figure 2 Schematic of the cascaded predictive control

This cascade structure is motivated for the present application from recognition of the fact that the system dynamics to be controlled by the high and low level controllers are of different natural time scales. The high level control must have sufficient response to control the lateral dynamics of a vehicle (within a typical bandwidth in the range of 1-3 Hz for road vehicles). The low level control must sufficiently control the individual tire/wheel dynamics whose bandwidth is higher (in the range of 5-20 Hz). With this separation, the low-level predictive control determines the individual wheel torques in such away as to balance the longitudinal tire saturations, while the high-level predictive control determines the corrective yaw moment to balance the lateral saturations.

Brief Review of MPC

Model predictive control involves using the system's model to predict the system's response to suitably parameterized future control inputs, and make optimization decisions that lead to the selection of the best control inputs that achieve some desired objective without violating constraints [22]. This is illustrated using Figure 3.

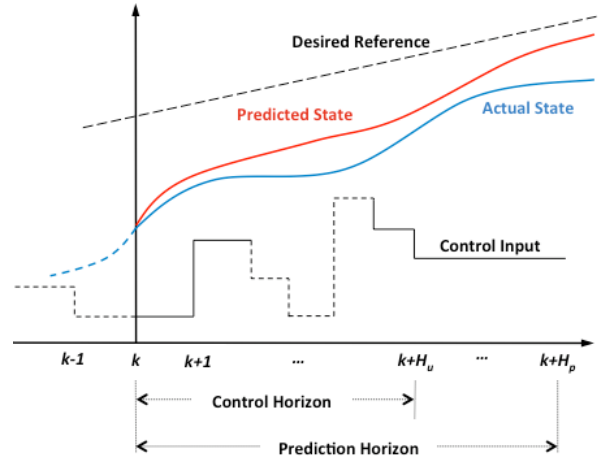


Figure 3 Model predictive control

The current time is denoted by index k . The prediction horizon, H_p , defines the time range in which the predicted state is optimized by variations of the control inputs that are restricted to change during the control horizon, H_u . In this work, we take the control horizon to be equal to the prediction horizon. MPC uses the system model to predict the future states (predicted states) that enter into optimization decisions to obtain the optimal control sequence that minimizes a defined optimization objective without violating constraints. A key aspect of MPC is that the optimization computations are repeated at each control update interval so that the most recent measurements (actual states) and model information could be used. In the present application, we use (nonlinear) MPC methods where in addition to new measurements (or state estimates for slip angles and tire forces), we use local linearization of the tire characteristics at each control update cycle.

Predictive Torque Distribution Control

For this low level control, we set the control objective as the optimal management of longitudinal tire force saturation levels among all tires. At first, a strategy that minimizes the total level of saturation across all tires might seem like a worthy objective. However, the presence of distinct longitudinal saturations is unavoidable when using differential braking/driving to achieve yaw stability corrections while meeting forward motion demands (of driver or forward speed control). In this work, an alternative objective of equalizing the saturation levels was conceived. The cost function for this objective is computed as the cumulative deviation of the individual longitudinal saturations from their average:

$$J = \left[\sum_{i=LF,RF,LR,RR} \left(\kappa_i - \frac{\sum_{j=LF,RF,LR,RR} \kappa_j}{4} \right)^2 \right] \quad (3)$$

This can be re-written in the usual quadratic matrix form as:

$$J = \bar{\kappa}^T Q_1 \bar{\kappa}, \quad Q_1 = \begin{bmatrix} 0.75 & -0.25 & -0.25 & -0.25 \\ -0.25 & 0.75 & -0.25 & -0.25 \\ -0.25 & -0.25 & 0.75 & -0.25 \\ -0.25 & -0.25 & -0.25 & 0.75 \end{bmatrix} \quad (4)$$

where, $\bar{\kappa}$ is a vector of the individual longitudinal tire saturations, and Q_1 is the constant positive semi-definite matrix as given.

The above objective function shall be used in a model predictive framework to solve for the optimal distribution of the individual wheel torques that minimizes this function subject to certain constraints. Namely, the individual wheel torques should satisfy the total base torque that is commanded by the driver (speed control) and the corrective yaw moment required by the predictive high-level controller to be detailed below. These online computed constraints are represented by:

$$\begin{bmatrix} \frac{d_f}{2} & \frac{d_f}{2} & -\frac{d_r}{2} & \frac{d_r}{2} \end{bmatrix} \begin{Bmatrix} F_{x,LF} \\ F_{x,RF} \\ F_{x,LR} \\ F_{x,RR} \end{Bmatrix} = M_\psi \quad (5)$$

$$\sum_{i=LF,RF,LR,RR} T_i = T_{total} \quad (6)$$

where, d_f and d_r are the track widths; R_w is the effective tire radius; $F_{x,i}$ is the individual wheel forces; M_ψ is the corrective yaw moment; T_i is the individual wheel torques; and T_{total} is the total base torque. Additional softer constraints on the increment of the wheel torques can be added to limit the rate change of the wheel torque to values achievable by the physical actuators/motors.

With the above, the MPC optimization problem can be cast in standard form as follows:

$$\min_{\Delta U} (Y^T Q Y + (\Delta U)^T R (\Delta U))$$

subjected to:

$$x_{k+1} = f(x_k, u_k, \Delta u_k)$$

$$\bar{\kappa}_{k+1} = g(x_{k+1}, u_k, \Delta u_k)$$

$$A_{eq} \Delta U = B_{eq}$$

$$Y = \begin{bmatrix} \bar{\kappa}_{k+1} \\ \vdots \\ \bar{\kappa}_{k+H_p} \end{bmatrix}; \quad \Delta U = \begin{bmatrix} u_{k+1} - u_k \\ \vdots \\ u_{k+H_u} - u_k \end{bmatrix}^T = \begin{bmatrix} \Delta u_k \\ \vdots \\ \Delta u_{k+H_p} \end{bmatrix}^T \quad (7)$$

where, the functions f and g define the predictive longitudinal vehicle and tire/wheel dynamics model (whose linearization is described below) with the longitudinal saturations κ as the system output; u is a vector of the four wheel torques; x is a vector of the system states that include the forward velocity, four wheel spins, and four longitudinal tire forces; Y is a system output matrix which is a concatenation of the individual tire saturations into the future prediction horizon; A_{eq} and B_{eq} are constant matrices that define the equality

constraints; Q and R are weighting matrices to be defined below.

A key parameter of the predictive framework is the prediction horizon whose selection should consider the specifics of the physical process. In the present case, the main considerations include a priori unknown future exogenous inputs, such as the driver inputs of steering and commanded base torque, and the uncertainty associated with the linearization of the vehicle and tire models. A remedy adopted here is to consider a short prediction horizon (of 0.1 seconds) implemented in a receding horizon scheme with fast update cycles (of 0.01 seconds) so the most recent information of these inputs can be used and the effects of the linearization errors can be minimized.

We now give the linearization adopted for the vehicle and tire model. For the forward vehicle dynamics:

$$\dot{V}_x = \frac{\sum_{i=LF,RF,LR,RR} F_{x,i} - \rho C_D S V_{x,0} V_x + \frac{1}{2} \rho C_D S V_{x,0}^2}{m} \quad (8)$$

where V_x is the vehicle's forward velocity, $F_{x,i}$ are the longitudinal tire forces; ρ is air density; C_D and S is the vehicle's drag coefficient and S frontal area; $V_{x,0}$ is the vehicle's velocity at the point of linearization (current state). For the tire/wheel rotational dynamics of each of the four tires:

$$\dot{\omega}_i = \frac{T_i - F_{x,i} R_w - b_i \omega_i}{I_w} \quad \text{for } i = LF, RF, LR, RR \quad (9)$$

where, the T_i is the controlled torque, R_w is the effective tire radius, and b_i is wheel viscous damping.

The longitudinal tire saturation defined earlier includes the longitudinal tire forces. It is desirable to formulate state equations for these forces. The longitudinal force dynamics can be constructed considering that these forces are functions of both the vehicle speed and tire/wheel spin. Then:

$$\dot{F}_{x,i} = \frac{\partial F_{x,i}}{\partial \sigma_i} \frac{\partial \sigma_i}{\partial \omega_i} \dot{\omega}_i + \frac{\partial F_{x,i}}{\partial V_x} \frac{\partial \sigma_i}{\partial V_x} \dot{V}_x = K_{1,i} \dot{\omega}_i + K_{2,i} \dot{V}_x \quad (10)$$

where, the coefficients K_1 and K_2 are determined from a nonlinear representation of the tire force/slip curve and partial derivatives of the slip ratio at the linearization point (given by $V_{x,0}$ and $\omega_{i,0}$). The gradient of the tire force with respect to slip ratio is a form of effective slip stiffness that can be implemented using a simple lookup table based on the current estimate of slip ratio (and possibly vertical load) at the linearization point. The look up table is to be obtained from tire test data or its analytical representations (e.g. Pacejka models).

The defining equations of the output longitudinal saturations are linearized at the current states as follows:

$$\kappa_i = -\frac{\omega_{i,0} R_w}{V_{x,0}^2} V_x + \frac{R_w}{V_{x,0}} \omega_i - \frac{1}{C_{xj}} F_{x,i} + \frac{\omega_{i,0} R_w - V_{x,0}}{V_{x,0}} \quad (11)$$

Equations (8)-(11) can be written in linear state space form and subsequently discretized for use as the predictive model for MPC. Details of these standard steps are given in [23]. To proceed, we write the resulting model in the form:

$$x_{k+1} = Ax_k + B_1 u_k + B_2 \quad (12)$$

$$y_{k+1} = Cx_k + E_1 \quad (13)$$

where, the matrices of A , B_1 , B_2 , C , and E_1 are updated based on the linearization of the system model at each control update cycle. Here, y is the output vector of the longitudinal saturations. A distinction of this process compared to standard MPC (e.g., [22]) is the presence of constant matrices B_2 and E_1 , which will eventually drop out of the optimization. By expanding the state and output vectors into the prediction horizon, the predicted outputs can be assembled:

$$\begin{aligned} \begin{Bmatrix} y_{k+1} \\ y_{k+2} \\ \vdots \\ y_{k+H_p} \end{Bmatrix} &= \begin{bmatrix} CA \\ CA^2 \\ \vdots \\ CA^{H_p} \end{bmatrix} x_k + \begin{bmatrix} CB_1 \\ CAB_1 + CB_1 \\ \vdots \\ \sum_{i=0}^{H_p-1} CA^i B_1 \end{bmatrix} u_{k-1} \\ &+ \begin{bmatrix} CB_1 & 0 & 0 & 0 \\ CAB_1 + CB_1 & CB_1 & 0 & 0 \\ \vdots & CAB_1 + CB_1 & \ddots & 0 \\ \sum_{i=0}^{H_p-1} CA^i B_1 & \sum_{i=0}^{H_p-2} CA^i B_1 & \cdots & CB_1 \end{bmatrix} \begin{bmatrix} \Delta u_k \\ \Delta u_{k+1} \\ \vdots \\ \Delta u_{k+H_p-1} \end{bmatrix} \\ &+ \begin{bmatrix} CB_2 \\ C2B_2 \\ \vdots \\ C(H_p-1)B_2 \end{bmatrix} + \begin{bmatrix} E_1 \\ E_1 \\ \vdots \\ E_1 \end{bmatrix} \end{aligned} \quad (14)$$

In compact form:

$$Y = \gamma x_k + \Omega u_{k-1} + \zeta \Delta U + \bar{E} \quad (15)$$

where Y and ΔU are concatenations of the predicted saturation outputs and wheel torque (control input) increments, respectively, through the prediction horizon; matrices γ , Ω , ζ , and \bar{E} are as given in Eq (14) and are constant during one control update/iteration; x_k and u_{k-1} are the current states and previous control inputs, respectively.

Substituting (15) in the optimization problem (7), expanding, simplifying, collecting terms, and neglecting constant additive terms, the optimization problem reduces to a quadratic form given by:

$$\begin{aligned} \min_{\Delta U} &\left\{ \begin{aligned} &(\Delta U)^T [\zeta^T Q \zeta + R] (\Delta U) \\ &+ [(\zeta x_k)^T Q \zeta + (\Omega u_{k-1})^T Q \zeta + \bar{E}^T Q \zeta \\ &+ (x_k \gamma Q)^T \zeta + (u_{k-1} \Omega Q)^T \zeta + (\bar{E} Q)^T \zeta] \Delta U \end{aligned} \right\} \\ &\text{subjected to:} \\ &A_{eq} \Delta U = B_{eq} \end{aligned} \quad (16)$$

where, the weighing matrix Q considers the saturation management objective (as concatenations of Q_1 given Eq(4)

into the prediction horizon); and R is a diagonal of control weights which affect the soft constraint on the rate of change of the input torques. The equality constraints of total torque and corrective yaw moment given previously ((5) and (6)) can be expressed in terms of the control input increment for the prediction horizon. The steps for doing this (i.e., for extracting A_{eq} and B_{eq} in (14)) are detailed in [23]. The optimization problem in (16) can be easily solved for the future wheel torque increments, ΔU , using quadratic optimization software tools. The MPC scheme updates this solution (including the linearization) at each control update cycle. For the torque distribution problem, this update is done at 100Hz (or every 0.01sec).

Predictive Yaw Moment Control

We incorporate the definition of axle lateral force saturation given earlier into an appropriate performance measure/objective function for the high-level of the cascade in Figure 2. Proceeding as before, the objective is set as one of minimizing the deviation of the lateral axle saturation levels from their average. The cost function is given by:

$$J = \left[\sum_{i=F,R} \left(\alpha_{sat,i} - \frac{\sum_{j=F,R} \alpha_{sat,j}}{2} \right)^2 \right] \quad (17)$$

This can then be rewritten in quadratic matrix form as:

$$J = \bar{\alpha}_{sat}^T Q_{\alpha,1} \bar{\alpha}_{sat} \quad Q_{\alpha,1} = \begin{bmatrix} 0.5 & -0.5 \\ -0.5 & 0.5 \end{bmatrix} \quad (18)$$

where, $Q_{\alpha,1}$ is a constant positive semi-definite matrix and $\bar{\alpha}$ is a vector of the lateral axle saturations. The optimization problem for the MPC is then posed as:

$$\begin{aligned} &\min_U \{ Y^T Q Y + U^T R U \} \\ &\text{subjected to:} \\ &x_{k+1} = p(x_k, u_k) \\ &y_{k+1} = q(x_k, u_k) \\ &U_{LB} < U < U_{UB} \\ &U = \begin{Bmatrix} u_k \\ \vdots \\ u_{k+H_u} \end{Bmatrix} = \begin{Bmatrix} M_{\psi,k} \\ \vdots \\ M_{\psi,k+H_u} \end{Bmatrix}; \quad Y = \begin{Bmatrix} \bar{\alpha}_{sat,k+1} \\ \vdots \\ \bar{\alpha}_{sat,k+H_u} \end{Bmatrix} \end{aligned} \quad (19)$$

where the functions p and q represent the lateral handling model of the vehicle used as the prediction model; U is the vector of corrective yaw moments over the control horizon H_u ; Y is the lateral axle saturations expanded into the prediction horizon H_p ; and U_{LB} and U_{UB} are the upper and lower bounds of the control input and limit the corrective yaw moment to physically achievable values.

There are two structural differences of this objective function compared to that of the torque distribution control problem of the previous section. First, the penalty weight, R , on

the control input is applied to the absolute magnitude of the control input but not to the increment of control. In our simulations, formulations including increment terms did not significantly improve performance. Furthermore, there is a fundamentally different goal in formulating the penalty in this manner. In the torque distribution control, it was desired to not significantly change the torque unless it was necessary, while in the present yaw moment control we penalize any magnitude of the corrective yaw moment (not just its increment). Secondly, there are no equality constraints for the present optimization to satisfy, but limiting values (bounds) are selected considering the capability of the vehicle to be controlled. The latter may also be functions of peak friction coefficients.

The predictive model we use for lateral handling dynamics is the usual single-track vehicle model at constant forward velocity:

$$\begin{aligned}\dot{V}_y &= \frac{(F_{yF} + F_{yR})}{m} - V_{x,0}\dot{\psi} \\ \dot{\psi} &= \frac{(F_{yF}l_f - F_{yR}l_r) + M_\psi}{J_z}\end{aligned}\quad (20)$$

where, V_y and $\dot{\psi}$ are the states of lateral velocity and yaw rate; the F_{yF} and F_{yR} are the front and rear axle lateral forces; m is the total vehicle mass; $V_{x,0}$ is the current estimate of the forward velocity; J_z is the yaw inertia; l_f and l_r are the distances from the vehicle's c.g. to the front and rear axle, respectively; M_ψ is a corrective yaw moment to be determined by the predictive control.

The lateral force is a nonlinear function of lateral velocity and yaw rate, which together define the axle slip angles. A simple first-order relaxation length model [24] was used to address the delay between the generation of lateral slip angle and the corresponding lateral force. Linearization of this force dynamics leads to:

$$\begin{aligned}\dot{F}_{y,F} &= \frac{V_{x,0}}{\lambda_F} \left[\frac{\partial f_{y,F}}{\partial \alpha} \Big|_{\alpha_{F,0}} \left(\frac{\partial \alpha_F}{\partial V_y} \Big|_{V_{y,0}} + \frac{\partial \alpha_F}{\partial \dot{\psi}} \Big|_{\dot{\psi}_0} - \delta \right) - F_{y,F} \right] \\ \dot{F}_{y,R} &= \frac{V_{x,0}}{\lambda_R} \left[\frac{\partial f_{y,R}}{\partial \alpha} \Big|_{\alpha_{R,0}} \left(\frac{\partial \alpha_R}{\partial V_y} \Big|_{V_{y,0}} + \frac{\partial \alpha_R}{\partial \dot{\psi}} \Big|_{\dot{\psi}_0} \right) - F_{y,R} \right]\end{aligned}\quad (21)$$

where, λ_F and λ_R are the front and rear relaxation lengths, respectively; $f_{y,F}$ and $f_{y,R}$ are the nonlinear functions describing tire lateral force versus slip angle; α_F and α_R are the front and rear axle slip angles, respectively; and δ is the road wheel steering angle (front steered vehicle). Substituting the definitions for the axle slip angles[25], the lateral axle force dynamics can be expressed in-terms of the yaw rate and lateral velocity:

$$\begin{aligned}\dot{F}_{y,F} &= \frac{V_{x,0}}{\lambda_F} \left(-C_1 \left(\frac{V_y + l_f \dot{\psi}}{V_{x,0}} - \delta \right) - F_{y,F} \right) \\ \dot{F}_{y,R} &= \frac{V_{x,0}}{\lambda_R} \left(-C_2 \left(\frac{V_y - l_r \dot{\psi}}{V_{x,0}} \right) - F_{y,R} \right)\end{aligned}\quad (22)$$

where, C_1 and C_2 are the partial derivatives of the tire force functions versus slip angle and represent the effective axle cornering stiffnesses at the operating points (current states). Again, these can be implemented through look up tables, and encompass a major simplification in the predictive model. They are to be updated at each iteration/update of the controller.

For the implementation of the lateral axle saturations in the objective function, it is desirable to have the axle saturations as outputs. From the definitions of axle saturation given by Eq (2), the linearized front and rear axle saturations are given as outputs of the state-space model as follows:

$$\begin{Bmatrix} \alpha_{sat,F} \\ \alpha_{sat,R} \end{Bmatrix} = \begin{bmatrix} \frac{1}{V_{x,0}} & \frac{l_f}{V_{x,0}} & -\frac{1}{C_1} & 0 \\ \frac{1}{V_{x,0}} & -\frac{l_r}{V_{x,0}} & 0 & -\frac{1}{C_2} \end{bmatrix} \begin{Bmatrix} V_y \\ \dot{\psi} \\ F_{yf} \\ F_{yr} \end{Bmatrix} + \begin{bmatrix} -\delta \\ 0 \end{bmatrix}\quad (23)$$

Using this linearized state space model, discretizing, and proceeding in similar steps as those used for the low level controller, the forward prediction can be written compactly as:

$$Y = \gamma x_k + \zeta U + \bar{E}\quad (24)$$

where Y is a concatenation of axle saturation levels through the prediction horizon; U is a vector of the corrective yaw moments for the horizon; the matrices of γ , ζ , and \bar{E} have similar interpretations as before. With these, the optimization problem for the high level control can be re-written as:

$$\begin{aligned}\min_U & \left\{ U^T [\zeta^T Q \zeta + R] U + [(\zeta x_k)^T Q \zeta + \bar{E}^T Q \zeta] \right. \\ & \left. + (x_k \gamma Q)^T \zeta + (\bar{E} Q)^T \zeta U \right\} \\ \text{subject to:} & \\ & U_{LB} < U < U_{UB}\end{aligned}\quad (25)$$

This formulation is different from standard MPC formulations[22] due to the constants (\bar{E}) in the prediction model, but it merely drops out of the optimization. The optimal control input U that minimizes the objective can be readily obtained through quadratic programming methods.

The control update interval for this high-level predictive control is chosen to be 0.1 sec and this is consistent with the short prediction horizon of the low-level control. The prediction horizon for the high-level MPC is chosen as 0.5 sec. For the optimizations conducted at each update, we assume that the remaining exogenous input (the steering input in the case of the high-level control) remains constant during the prediction horizon. Simulations suggest that the faster control updates (every 0.1 sec) help compensate for limitations of this assumption.

RESULTS AND DISCUSSIONS

Test Vehicle and Maneuver

For the purpose of demonstrating the performance of the proposed cascaded predictive saturation management strategy, we applied the strategy to a simulation model of a medium duty truck with a GVW of 8000 lbs and with a powertrain featuring independent wheel drives. This vehicle has a high center of gravity and easily approaches oversteer conditions during transient maneuvers on dry ($\mu_{\text{peak}}=1.0$) asphalt road. The mathematical vehicle model exercised in these analysis is described elsewhere[20]. We also adopt an open-loop “sine with dwell” maneuver that has been defined by NHTSA in the US to emulate a severe obstacle avoidance type maneuver for the purpose of evaluating VSC systems. This input induces a dynamic nonlinear response featuring high sideslip for the uncontrolled vehicle. The steering input and the trajectory response for the uncontrolled and controlled vehicle are shown in Figure 4.

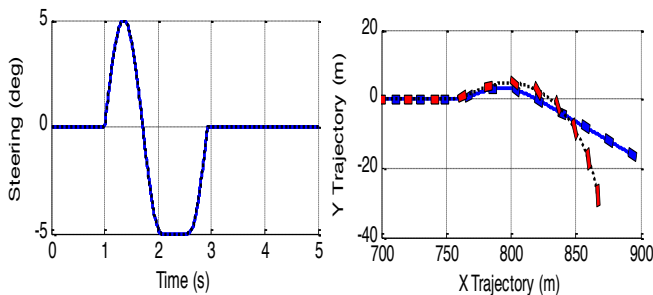


Figure 4 Road wheel steering input and controlled (blue) and uncontrolled (red) open-loop vehicle trajectory

Performance of the Cascaded Predictive Stability Control

We first show the two inputs computed online by the high-level controller (corrective yaw moment) and the forward speed controller (or driver base torque) and passed as constraints for the low-level controller. During the maneuver, the vehicle speed is inevitably reduced due to the effects of lateral tire force components on the longitudinal dynamics of the vehicle. To limit the effect of the speed restoring action of the speed controller, the total drive (base) torque has been limited to 500 Nm in this example (Figure 5). However, it should be recognized that in some traction control systems the base torque is also actively reduced. We neglected this aspect to maintain the focus on the proposed strategy.

For the purpose of comparison, we consider a traditional PI-type yaw rate reference controller [2, 20] to substitute the high-level predictive yaw moment controller of the cascade structure. We keep the low-level torque distribution controller the same for both. Figures 6 and 7 show some comparisons of the responses.

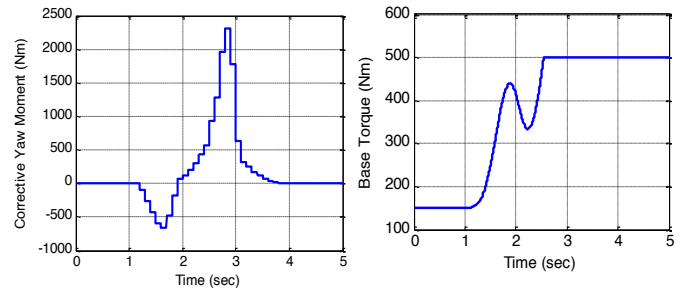


Figure 5 Online constraints for the low-level controller using predictive yaw control

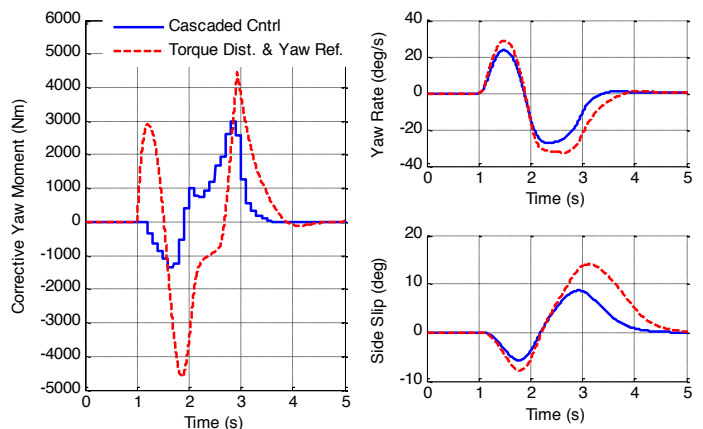


Figure 6 Comparison of yaw-reference and cascaded predictive control

It should be noted that the two high-level controllers in this comparison seek to accomplish two separate goals. The goal of the traditional yaw rate reference controller is to force the vehicle to obtain the desired yaw rate determined by a steady-state yaw-rate gain. This controller does not take into consideration the lateral force capability of the individual axles, and consequently induces higher vehicle sideslip. However, the cascaded predictive control proposed here seeks to achieve a balance of lateral axle saturations and to use the lateral force capacity of each axle evenly. Due to the oversteering nature of the example vehicle, the predictive control adds stabilizing moment to reduce rear axle saturation, as seen during the initial part of the maneuver (Figure 6 left). Conversely, the yaw reference controller accepts more transient oversteer and applies a yaw moment to induce more response in an effort to approach the desired yaw rate.

It is also observed that the cascaded predictive control uses less actuation effort to achieve improved performance. This is evident in the corrective yaw moment needs in Figure 6 and the individual wheel torques from the low-level optimal torque distribution control as shown in Figure 7. We attribute this reduced need for actuation effort to the more efficient/balanced use of the available traction capability of all tires.

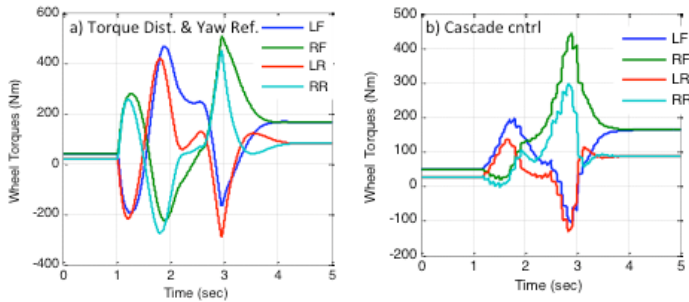


Figure 7 Optimal wheel torques under the two high-level controllers

CONCLUSIONS

In this paper, we outlined a cascaded predictive control structure that manages tire force saturation for the purpose of directional stability control of road vehicles. The approach has been successfully applied to a simulation model of a medium duty truck, where balancing saturation is shown to stabilize the vehicle with reduced actuation effort in independent drive configurations. We remark that, with some modifications of the constraints, it is possible to extend the approach to torque vectoring differentials and brake-based VSC systems.

Finally, it should be noted that the approach proposed here relied on knowledge of the tire's force generation model, particularly the availability of look-up tables of the cornering and slip stiffness characteristics with the prevailing slip quantities. Further work will pursue identification schemes that address this and other issues related to accommodating variability of tire characteristics with load and friction conditions within the cascaded predictive optimal control scheme.

REFERENCES

- [1] T. VanZanten, "Bosch ESP Systems: 5 Years of Experience", in SAE Automotive Dynamics & Stability Conference, SAE Paper No. 2000-01-1633.
- [2] H. E. Tseng, B. Ashrafi, D. Madau, T. Allen Brown, and D. Recker, "The development of vehicle stability control at Ford". IEEE/ASME Transactions on Mechatronics, 1999. 4(3): p. 223-234.
- [3] A. Goodarzi and E. Esmailzadeh, "Design of a VDC System for All-Wheel Independent Drive Vehicles". IEEE/ASME Transactions on Mechatronics, 2007. 12(6):p.632-639.
- [4] E. Esmailzadeh, A. Goodarzi and G.R. Vossoughi,G "Optimal yaw moment control law for improved vehicle handling". Mechatronics, 2003. 13(7): p. 659-675.
- [5] I. Karogal and B. Ayalew, "Independent Torque Distribution Strategies for Vehicle Stability Control," SAE Paper No.2009-01-0456.
- [6] R. P. Osborn and T. Shim, "Independent Control of All-Wheel-DriveTorque Distribution". SAE Paper No..2004-01-2052.
- [7] F. Borrelli, M. Baotic, J. Pekar, and G. Stewart, "On the computation of linear model predictive control laws". Automatica. 46(6): p. 1035-1041.
- [8] P. Falcone, F. Borrelli, J. Asgari, H.E. Tseng, and D. Hrovat, "Predictive Active Steering Control for Autonomous Vehicle Systems". IEEE Transactions on Control Systems Technology, 2007. 15(3): p. 566-580.
- [9] P. Falcone, M. Tufo, F. Borrelli, J. Asgari, and H.E. Tseng. "A linear time varying model predictive control approach to the integrated vehicle dynamics control problem in autonomous systems". 2008. Piscataway, NJ, USA: 2980-5, IEEE.
- [10]P. Falcone, H. Eric Tseng, F. Borrelli, J. Asgari, and D. Hrovat, "MPC-based yaw and lateral stabilization via active front steering and braking". Vehicle System Dynamics: International Journal of Vehicle Mechanics and Mobility, 2008. 46(1): p. 611 - 628.
- [11]Z. HongLiang and L. ZhiYuan. "Design of vehicle yaw stability controller based on model predictive control". In IEEE Intelligent Vehicles Symposium. June 3-5,2009, p. 802-807.
- [12]F. Borrelli, A. Bemporad, M. Fodor, and D. Hrovat, "An MPC/Hybrid System Approach to Traction Control". IEEE Trans. Control System Technology, 2006. 14(No. 3): p. pp. 541-552.
- [13]J. Kim, "Identification of lateral tyre force dynamics using an extended Kalman filter from experimental road test data". Control Engineering Practice, 2009. 17(3): p. 357-367.
- [14]Y. Fukada, "Slip-Angle Estimation for Vehicle Stability Control". Vehicle System Dynamics: International Journal of Vehicle Mechanics and Mobility, 1999. 32(4): p. 375 - 388.
- [15]L. R. Ray, "Nonlinear state and tire force estimation for advanced vehicle control". Control Systems Technology, IEEE Transactions on, 1995. 3(1): p. 117-124.
- [16]L. R. Ray, "Nonlinear Tire Force Estimation and Road Friction Identification: Simulation and Experiments". Automatica, 1997. 33(10): p. 1819-1833.
- [17]D. Piyabongkarn, J.Y. Lew, R. Rajamani, J.A. Grogg, and Y. Qinghui, "On the Use of Torque-Biasing Systems for Electronic Stability Control: Limitations and Possibilities". Control Systems Technology, IEEE Transactions on, 2007. Vol. 15(No. 3): p. 581-589.
- [18]M. Gradu, "Torque Bias Coupling for AWD Applications". SAE Paper No. 2003-01-0676.
- [19]J. Limroth, "Real-time Vehicle Parameter Estimation and Adaptive Stability Control", 2009, Clemson University, Ph.D. Dissertation in Automotive Engineering, Clemson, SC.
- [20]J. Sill and B. Ayalew, "A Saturation Balancing Control Method for Enhancing Dynamic Vehicle Stability". Int. J. of Vehicle Design, Vol. 61, Nos. 1/2/3/4, pp. 47-66, 2012 .
- [21]J. Sill and B. Ayalew "Vehicle Stability Control Through Predictive and Optimal Tire Saturation Management", in 14th International Conference in Advanced Vehicle

- Technologies, Proceedings of the ASME IDETC/CIE-2012, Chicago, IL, August 12-15. DETC2012-71182.
- [22] J. M. Maciejowski. Predictive Control with Constraints. 2002, Prentice Hall: Harlow, England.
- [23] J. Sill, "Predictive Tire Force Saturation Management for Vehicle Stability Control". 2012, Clemson University, Ph.D. Dissertation in Automotive Engineering, Clemson, SC.
- [24] G. Rill, "First Order Tire Dynamics", in 3rd European Conference on Computational Mechanics. June 5-8, 2006, Lisbon, Portugal.
- [25] G. Genta, Motor Vehicle Dynamics: Modeling and Simulation. Series on Advances in Mathematics for Applied Sciences. Vol. 43. 1997, Singapore, World Scientific Publishing.